Graphic Analysis of Perturbed Rydberg Series*

K. T. Lu and U. Fano
Department of Physics, The University of Chicago, Chicago, Illinois 60637
(Received 19 January 1970)

A method of analysis of all level positions in multiple strongly perturbed series of levels is presented and illustrated by examples from the rare gas and Ba spectra. The method is suggested by Seaton's multichannel quantum defect theory but is presented here as an empirical approach. It emphasizes the dependence of a perturbation on the periodicity of the perturbing series and aims at extracting significant information from experimental data in compact form; this goal will be pursued in later works.

Treatments of the configuration interaction of two (or more) mutually perturbing series currently utilize the Shenston-Russell-Edlén formula,[1] which derives from a second-order perturbation theory by Langer.[2] They also utilize plots of the quantum defect $\mu = n - n^*$ against term value T_n. These plots show an irregularity, similar to an anomalous dispersion curve, wherever a perturbing level of another series occurs in the spectrum. This formalism maintains a clear distinction between a foreign perturbing level, or series of levels, and the perturbed series. If the foreign level were counted among those of the perturbed series, all higher levels of this series would be assigned a value of n one unit higher.

However, this distinction between the two series becomes somewhat artificial when configuration interaction cannot be adequately described by second-order perturbation effects and the wave function of a perturbing level becomes strongly admixed into many levels of the perturbed series. Moreover, plotting μ against T_n fails to emphasize the periodicity of the perturbing series and its convergence to a different limit, beyond that of the perturbed series.

These limitations of the current treatments are overcome, in principle, by Seaton's multichannel quantum defect theory.[3] Efforts have been underway for some time[4] to extend the applications of this theory to extract a maximum of information from experimental data. At this time, it seems useful to present here a graphical method of manipulating data which displays and utilizes simultaneously the Rydberg character of different series and will prove useful for further developments. These developments will be reported later,[5,6] but some of their results will be anticipated here. This paper presents an empirical approach for the analysis of experimental data, but postpones a full explanation of its theoretical basis.

Quantum defect theories express the eigenvalue equation for the discrete levels of a Rydberg series by an equation of the type

$$\sin\pi(\nu_n + \mu) = 0 . \tag{1}$$

Here ν_n (often called n^*) is the effective quantum number of a level and μ is the quantum defect, which is approximately constant for a whole Rydberg series in the absence of perturbation. The solutions of (1) are, of course,

$$\nu_n = n - \mu . \tag{2}$$

The Shenstone-Russell-Edlén formula makes μ apparently singular at the spectral location of each separate perturbing level. This paper presents evidence showing that μ is conveniently plotted as a monotonically increasing function of energy which exhibits the Rydberg periodicity of the perturbing series. Moreover, this periodicity is brought out most clearly by plotting together the μ values of all perturbed series which converge to the same limit.

It has been known for a long time[7] that the quantum defect of a Rydberg series extrapolates in the continuum beyond the series limit into the phase shift of the electron-ion scattering problem according to the formula

$$\delta = \pi\mu . \tag{3}$$

The multichannel theory[3] extends this connection, δ being an eigenphase shift of the scattering problem. The plots of μ shown here and in earlier literature[8] exhibit the series perturbations in the form familiar from the theory of resonance scattering.[9]

As a first illustration we consider a "multichannel" system, that is, an atom with several series, some of which converge to the ground state and some to an excited state of an ion. Photoabsorption by Xe in its ground state leads to p^5d or p^5s, $J = 1$, odd-parity states belonging to five series, of which three, called[10] $5p^5(^2P_{3/2})ns[1\frac{1}{2}]^\circ$, $5p^5(^2P_{3/2})nd[\frac{1}{2}]^\circ$, $5p^5(^2P_{3/2})nd[1\frac{1}{2}]^\circ$, converge to the first ionization potential $T_{1\infty}$ and two, $5p^5(^2P_{1/2})ns'[\frac{1}{2}]^\circ$, $5p^5(^2P_{1/2})nd'[1\frac{1}{2}]^\circ$, converge to a second ionization potential $T_{2\infty}$. It is usually said

that the first three series are perturbed by members of the last two series. Here we do not distinguish initially between the "perturbed series" and the "perturbing level," or even between level series converging to the same limit. Instead, we consider equally all experimental levels T_m, with $J=1$ and odd parity, below the first limit $T_{1\infty}$; to each of them we assign *two* alternative effective quantum numbers ν_1 and ν_2 defined, respectively, by the equations

$$T_m = T_{1\infty} - R/\nu_{1m}^2, \tag{4a}$$

$$T_m = T_{2\infty} - R/\nu_{2m}^2, \tag{4b}$$

where R is the Rydberg constant. These equations imply the functional relation between ν_1 and ν_2,

$$\nu_1 = \nu_2/(1-\nu_2^2\,\Delta)^{1/2}, \quad \Delta = (T_{2\infty} - T_{1\infty})/R. \tag{5}$$

We also assign to each level T_m a single quantum defect

$$\mu_m = n - \nu_{1m}, \tag{6}$$

where n is an integer shown in Fig. 2(a), which may have the same value for two (or more) levels; we shall usually plot only the decimal part of μ, i.e., we plot μ *modulo* 1, except for some extrapolation to display periodicities.

Values of μ_m for the 28 levels available for Xe[10] are thus plotted in Fig. 1 against ν_{2m}. To emphasize the connection with usual practice, the 25 points (μ_m, ν_{2m}) usually assigned to series converging to $T_{1\infty}$ are marked by open circles, and the three points usually assigned to series converging to $T_{2\infty}$ are marked by ×. The solid and dashed lines joining the points are interpolated curves which represent all quantum defects as points lying on the plot of a *multivalued continuous function* $\mu(\nu_2)$. In terms of this continuous function, Eqs. (4a), (4b), and (2) imply together that the observed levels are determined as the roots of the equation, analogous to (1),

$$\sin\pi[\nu_1 + \mu(\nu_2)] = 0. \tag{7}$$

In this paper $\mu(\nu_2)$ is regarded as an empirical function. The connection of this equation with Seaton's theory is outlined in the Appendix. As shown in Fig. 2(a), Eq. (7) requires each point (μ_m, ν_{2m}) to lie at an intersection of the curve $\mu(\nu_2)$ and of a plot *modulo* 1 of the function $\nu_1(\nu_2)$ defined by (5).

Key properties of $\mu(\nu_2)$ are apparent by inspection of Fig. 1, but are brought out more clearly by constructing the corresponding graph for Ar [Fig. 2(a)]. This construction has recently been made possible by extensive new data.[11] Most of the available points are concentrated in the interval $8.0 < \nu_2 < 8.4$ near the $T_{1\infty}$ limit. The remaining

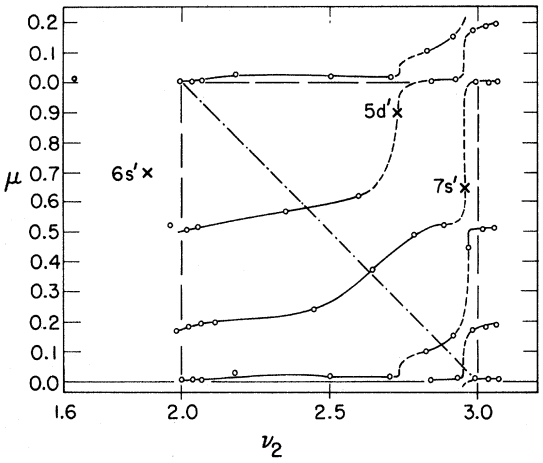

FIG. 1. The quantum defect μ-versus-ν_2 plot of Xe. Open circles (o) are level positions of the three series $p^5(^2P_{3/2})ns[1\frac{1}{2}]^\circ$, $p^5(^2P_{3/2})nd[\frac{1}{2}]^\circ$, and $p^5(^2P_{3/2})nd[1\frac{1}{2}]^\circ$. Crosses (×) labeled nl' correspond to level positions of the two series $p^5(^2P_{1/2})ns'[\frac{1}{2}]^\circ$ and $p^5(^2P_{1/2})nd'[1\frac{1}{2}]^\circ$. Solid and dashed lines are interpolated with varying degree of confidence. A diagonal dot-dash line represents the equation $\mu(\nu_2)+\nu_2=1$. The curves outside the basic unit square are the repeated portions of those within the square.

67 points might not quite suffice to draw the curves $\mu(\nu_2)$ with reasonable assurance, were it not for the clear pattern of periodicity in ν_2. (This periodicity is less clear in Fig. 1, where most data fall in a unit range of ν_2.) The periodicity is utilized in Fig. 2(b), where the data of Fig. 2(a) are replotted *modulo* 1, i.e., with successive unit intervals of ν_2 folded onto one another. The points corresponding to such different intervals are now seen to interpolate rather smoothly to define a single multibranched periodic curve $\mu(\nu_2)$.

Inspection of both Figs. 1 and 2(b) reveals now the key point of this paper, namely, that $\mu(\nu_2)$ is a periodic function of ν_2. One may also consider $\mu(\nu_2)$ as defined implicitly by an equation $F(\mu, \nu_2) = 0$, where F is a periodic function of both μ and ν_2 (see Appendix). Thereby each branch of the curve which exits from one margin of the basic unit square of the plot reappears at the corresponding point of the opposite margin. If one regards such corresponding points on opposite margins as the "same" point, all branches of the curve in each figure are seen to be parts of a single continuous curve. In our example, where three "series" converge to $T_{1\infty}$ and two to $T_{2\infty}$, any vertical line drawn across the basic unit square intersects $\mu(\nu_2)$ three times and any horizontal line intersects it two times.

The theory of unperturbed Rydberg series relies on the possibility of introducing a quantum defect μ which is nearly constant as the energy of succes-

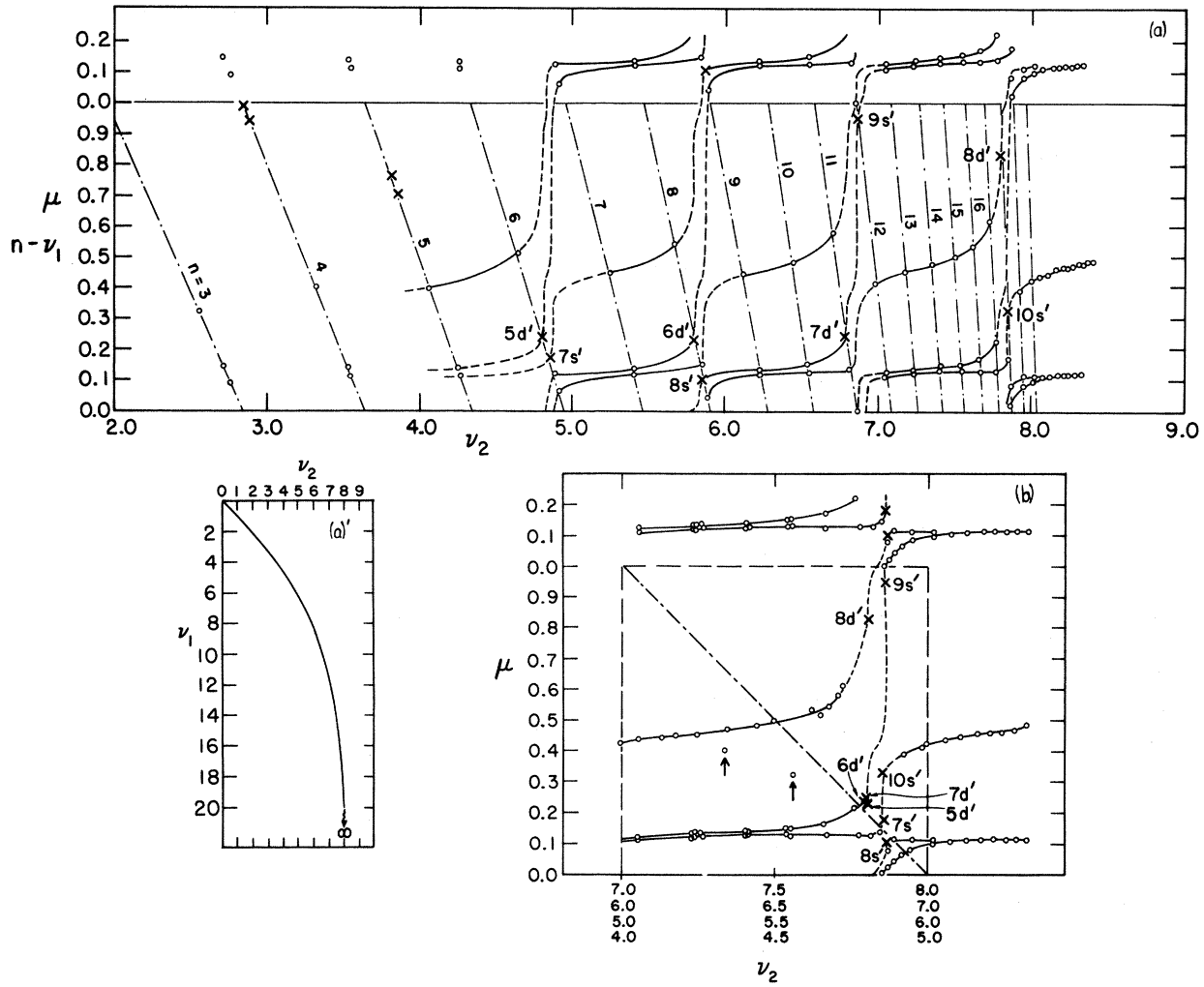

FIG. 2. (a) The quantum defect μ-versus-ν_2 plot of Ar. Open circles and cross marks as in Fig. 1. No interpolated curves are drawn for $\nu_2 < 4$ because points are too sparse. The function $-\nu_1(\nu_2)$ defined by Eq. (5) is shown in the box (a)′ and again, *modulo* 1, by a dot-dash line. Numerical labels on these curves indicate values of integer n of Eq. (6). (b) The folded quantum defect μ-versus-ν_2 plot of Ar. The data of (a) with $\nu_2 > 4.0$ are replotted with ν_2 scale *modulo* 1, i.e., with successive intervals of ν_2 folded onto one another. Some points with $\nu_2 < 4.0$ are included (†) to show departure from the interpolated curves.

sive levels varies along the spectrum. (Minor variations of μ for the lower levels of a series are commonly observed and taken for granted.) Here, we have introduced the *function* $\mu(\nu_2)$ which is similarly understood to be nearly, but not quite, periodic along the spectrum. In Fig. 1, three points lie at $\nu_2 < 2$; shift of each of these points by one unit of the abscissas brings each of them close to — but not quite on — one branch of the curve $\mu(\nu_2)$. Similarly, Fig. 2(a) includes a number of points with $\nu_2 < 4$; some of these points are those that appear in Fig. 2(b) at substantial distance from the curves.

The crosses, which represent levels usually assigned to "perturbing" series lie on sharply rising portions of the curves. Indeed, if all interactions between series were very weak, all unperturbed levels of the "perturbed" series would be represented by circles lying on flat portions of the curves, i.e., with constant μ values. The flat portions would be separated by sharp steps and pairs of curves would nearly touch each other at the step corners. Some of the curves in Figs. 1 and 2 actually rise quite sharply, leaving small gaps at the corners, other steps are smoother; in some instances no reasonably flat, i.e., unperturbed, portion of curve is seen. The magnitude of the gaps between successive curves provides a visual estimate of the strength of the interaction between different series.

Proceeding now to a more detailed analysis of data, one notes in Fig. 1 a number of points with nearly the same quantum defect $\mu_1 \simeq 0.0$. This set of points represents the $5p^5(^2P_{3/2})ns[1\frac{1}{2}]^\circ$ channel according to Moore's assignment. Among the other points one can roughly single out two groups with quantum defects $\mu \cong 0.5$ and 0.18, respectively. These two sets of points represent levels labeled[10] $5p^5(^2P_{3/2})nd[\frac{1}{2}]^\circ$ and $5p^5(^2P_{3/2})nd[1\frac{1}{2}]^\circ$, respectively. However, they belong neither purely to $nd_{3/2}$ nor to $nd_{5/2}$; most of them being also appreciably perturbed. Their character remains to be determined in a separate paper.[6] Since the level usually labeled $p^5P_{1/2}5d'$ lies at $\nu_2 = 2.73$, the appearance of the curves indicates that this level interacts strongly with $P_{3/2}s$. The $p^5P_{1/2}7s'$ level, which lies at 2.95, interacts less strongly, mostly with $P_{3/2}d[\frac{1}{2}]$ and less so with $P_{3/2}d[1\frac{1}{2}]$ and $P_{3/2}s_{1/2}$. (Incidentally, it had been previously suggested[12] that s' levels would interact mostly with $P_{3/2}s_{1/2}$.) The pair of steps in the curves between $\nu_2 = 2.6$ and 3.0 resembles the steps that would be observed in scattering-phase plots in the region of two somewhat overlapping resonances. In the scattering problem the sum of the phases of all open channels increases by π at each resonance; here the sum of the three μ values increases by unity.[13]

The unperturbed part of the $nd[1\frac{1}{2}]^\circ$ series of Ar [Figs. 2(a) and 2(b)] is almost degenerate with the $ns[1\frac{1}{2}]^\circ$ series unlike the corresponding series of Xe. The levels of the "perturbing" series $p^5P_{1/2}nd'$ lie at $\nu_2 = 4.81$, 5.80, 6.79, and 7.8, corresponding to $n = 5$, 6, 7, and 8, respectively. The appearance of the curves indicates that this series interacts strongly with the series $P_{3/2}d[\frac{1}{2}]^\circ$, less strongly with $P_{3/2}d[1\frac{1}{2}]^\circ$, and very weakly with $P_{3/2}s[1\frac{1}{2}]^\circ$. The levels of the "perturbing" series $p^5P_{1/2}ns'$, which lie at $\nu_2 = 4.85$, 5.87, 6.86, and 7.85, corresponding to $n = 7$, 8, 9, and 10, respectively, interact less strongly with $P_{3/2}s[1\frac{1}{2}]^\circ$ and very weakly with $P_{3/2}d[\frac{1}{2}]^\circ$ and $P_{3/2}d[1\frac{1}{2}]^\circ$. The fact that the interaction between the d and s series is so weak was also noted by Yoshino.[11]

For Kr we have only a limited amount of data,[14] which are plotted for purposes of orientation and comparison in Figs. 3(a) and 3(b). The lower levels are not adequate to construct good interpolated curves in Fig. 3(a), nor do they fit well the folded plot in Fig. 3(b). The analysis may be improved when higher levels become available experimentally. The curve pattern of Kr shows characteristics intermediate between those of Ar and Xe. There is no degeneracy among series as in Ar. The curves also show the two stepwise jumps and an interaction between d and s series which is larger than in Ar and smaller than in Xe.

A final illustration, Fig. 4 shows a $\mu(\nu_2)$ plot for the single principal series $(6smp^1P_1^\circ)$ of Ba.[15] As $T_{1\infty}$ we take, of course, the series limit $6s^2S_{1/2}$, and as $T_{2\infty}$, we take somewhat arbitrarily the series limit $5d^2D_{5/2}$, to which the series $5dmp^1P_1^\circ$ converges. Here the interpolated curve of the principal series jumps, in essence, by one unit of μ whenever it passes through one of the perturbing levels $5d6p^1P_1^\circ$, $5d8p^1P_1^\circ$, $5d8p^3D_1^\circ$, and $5d8p^3P_1^\circ$, which are marked by × in the graph. Note how the points corresponding to $6smp^1P_1^\circ$ with $m = 6$, 7, 8, and 9 lie rather well, but not perfectly, along the line determined by higher m values. In fact the plot serves to call attention to possibly aberrant data. In particular, the point corresponding to the level called by Garton[15] $5d4f^1P_1^\circ$ (?) does not seem to be in the right place. The levels $5d8p^3D_1^\circ$ and $5d8p^3P_1^\circ$ actually belong to series converging to the limit $5d^2D_{3/2}$

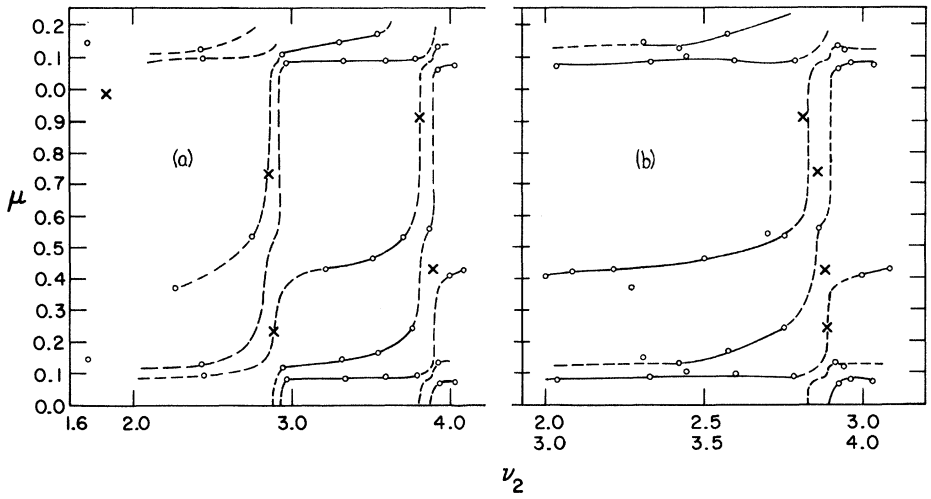

FIG. 3. (a) The quantum defect μ-versus-ν_2 plot of Kr. Because of the sparse distribution of the points the interpolated curves are sketched most tentatively. (b) The data of (a) with $\nu_2 > 2.0$ replotted *modulo* 1. The tentative interpolated curves are drawn through the points with $\nu_2 > 3.0$.

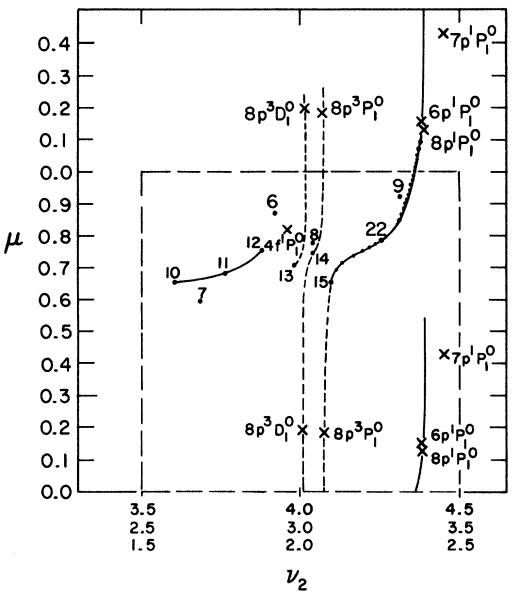

FIG. 4. The quantum defect μ-versus-ν_2 plot of Ba. Dot numbers indicate the n value of principal series $6snp\,^1P_1^\circ$ levels. Crosses labeled $nl^{1,3}L_1^\circ$ correspond to $5dnl^{1,3}L_1^\circ$.

of Ba^+, which lies somewhat below $T_{2\infty}$ ($5d^2D_{5/2}$ of Ba^+). The extension of the present paper, to take into account the occurrence of three or more series limits, remains to be explored.

We wish, however, to indicate some of the directions of the investigation now in progress.[6] Line strengths and g factors may be plotted as periodic functions of ν_2, showing systematic variations related to those of $\mu(\nu_2)$. The intensity plots extrapolate into the Beutler spectra of the continuum (see, e.g., Fig. 28 of Ref. 16). A point of particular interest concerns the intersections of $\mu(\nu_2)$ curves with the $\mu(\nu_2)+\nu_2 = 1$ diagonal lines shown in Figs. 1 and 2(b).[5] States of the atom represented by points close to these intersections are approximately eigenstates of the scattering problem of one electron colliding with a ground state or excited ion core with near-zero energy; the μ values at the intersections represent, to within a factor of π, the eigenphases of this scattering problem.

We emphasize in conclusion that the curves in the graphs of this paper have no claim to accuracy. They have been drawn somewhat sketchily for purposes of illustration; more accurate determinations should follow. Eventually the approach outlined here might be utilized by experimenters interested in specific spectra.

APPENDIX: CONNECTION WITH SEATON'S THEORY

The levels T_m of a discrete spectrum are determined in Ref. 3 through the roots of the determinant Eq. (7), namely,

$$|\tan\pi\nu + \underline{R}| = 0. \qquad \text{(A1)}$$

Here $\underline{R}$ is a reaction matrix which varies slowly as a function of energy and ν is a matrix whose eigenvalues $\nu_\alpha = \nu_1, \nu_2, \ldots,$ are related to one another and to the energy E by the equation analogous to our Eq. (4):

$$E/hc = T_{1\infty} - R/\nu_1^2 = T_{2\infty} - R/\nu_2^2 \cdots$$
$$= T_{\alpha\infty} - R/\nu_\alpha^2 = \cdots, \qquad \text{(A2)}$$

the $T_{\alpha\infty}$ being levels of the ion core spectrum ($T_{1\infty} \leq T_{2\infty} \leq \cdots$). Equation (A1) is an eigenvalue equation because the ν_α are all related to one another. (In the main text of this paper, with reference to rare gases a single symbol ν_1 has been used to indicate three degenerate eigenvalues while $\nu_\alpha\,\nu_2$ has been used for the other two values.)

To connect Seaton's work[17] with the empirical procedure of this paper we envisage the solution of (A1) by a two-step parametric procedure. In the first step we *replace* in (A1) the elements ν_1 of the diagonalized matrix ν by a parameter $-\mu$. The equation thus obtained then defines μ as an implicit function $\mu(\nu_2 \cdots \nu_\alpha \cdots)$ of all elements of ν with $\alpha > 1$; this definition holds for any value of the energy E. [This paper actually determines the same function μ by interpolation of experimental data rather than from implied knowledge of $\underline{R}$ and solution of the modified equation (A1).] The next step of the procedure consists of seeking those values of ν_1 related to $\nu_2 \cdots \nu_\alpha \cdots$ by (A2), which fulfill with $\mu(\nu_2 \cdots \nu_\alpha \cdots)$ the eigenvalue equation

$$\tan\pi[\nu_1 + \mu(\nu_2 \cdots \nu_\alpha \cdots)] = 0, \qquad \text{(A3)}$$

equivalent to (7).

---

*Work supported by the U. S. Atomic Energy Commission, under Contract No. COO-1674-27.

[1]B. Edlén, *Encyclopedia of Physics* (Springer-Verlag, Berlin, 1964), Vol. 27, p. 80.
[2]R. Langer, Phys. Rev. 35, 649 (1930).
[3]M. J. Seaton, Proc. Phys. Soc. (London) 88, 801 (1966).
[4]K. T. Lu, Bull. Am. Phys. Soc. 13, 37 (1968).
[5]U. Fano (unpublished).
[6]K. T. Lu (unpublished).
[7]See, for example, M. J. Seaton, Monthly Notices Roy. Astron. Soc. 118, 504 (1958).

[8]See, for example, M. J. Seaton, Proc. Phys. Soc. (London) 88, 815 (1966); and D. L. Moores, *ibid.* 88, 843 (1966).

[9]P. G. Burke and H. M. Schey, Phys. Rev. 126, 147 (1962). This fact is also well known in nuclear and particle physics.

[10]C. E. Moore, *Atomic Energy Levels* (U. S. Natl. Bur. Std., Washington, D. C., 1958), Circ. No. 467, Vol. III.

[11]K. Yoshino, Optical Society of America 1969 Annual Meeting program No. WH12 (unpublished); K. Yoshino (unpublished). (We express our appreciation to Dr. Yoshino for allowing us full use of the data before formal publication.)

[12]H. Beutler, Z. Physik 93, 177 (1935); F. J. Comes and H. G. Sälzer, Phys. Rev. 152, 29 (1966).

[13]J. Macek, Phys. Rev. A 1, 618 (1970); and see, for example, P. G. Burke, J. W. Cooper, and S. Ormonde, *ibid.* 183, 245 (1969).

[14]Reference 10, Vol. II (1952).

[15]W. R. S. Garton and K. Codling, Proc. Phys. Soc. (London) 75, 87 (1960); W. R. S. Garton and F. S. Tomkins, Astrophys. J. 158, 1219 (1969).

[16]U. Fano and J. Cooper, Rev. Mod. Phys. 40, 441 (1968).

[17]M. J. Seaton, J. Phys. B2, 5 (1969).

PHYSICAL REVIEW A VOLUME 2, NUMBER 1 JULY 1970

Experiments on the 2^3P State of Helium. II. Measurements of the Zeeman Effect*

S. A. Lewis,† F. M. J. Pichanick,‡ and V. W. Hughes

Physics Department, Yale University, New Haven, Connecticut 06520

(Received 17 December 1969)

A series of Zeeman resonances has been measured in the 2^3P state of He^4, using the optical-microwave atomic-beam magnetic-resonance technique. The results were analyzed in terms of relativistic and motional contributions to the Zeeman effect, and are presented in the form of corrected g factors: $g_{S'} = g_S - (76.0 \pm 2.4) \times 10^{-6}$, $g_{L'} = g_L + (3.8 \pm 9.0) \times 10^{-6}$, and an additional factor $g_x = (4.0 \pm 25.0) \times 10^{-6}$. These are compared with theoretical calculations using quasi-hydrogenic radial wave functions which give $g_{S'} = g_S - (79.9 \pm 3.5) \times 10^{-6}$, $g_{L'} = g_L + (1.1 \pm 1.5) \times 10^{-6}$, and $g_x = -(3.2 \pm 4.4) \times 10^{-6}$. The values of the experimental g factors are $g_S^1 = 2.002\,243\,2 \pm 0.000\,022\,4$, and $g_L^1 = 0.999\,867 \pm 0.000\,009$. The validity of the theory and the consistency of the data are discussed. The experimental results were used to reduce the quoted uncertainty in a previously reported fine-structure measurement. The new result is $E(2^3P_1) - E(2^3P_2) = 2291.196 \pm 0.005$ MHz.

I. INTRODUCTION

A previous paper[1] (referred to as I) reported a measurement of the $2^3P_1 - 2^3P_2$ fine-structure interval of helium to a precision of 3 ppm. The most accurate data were taken in a magnetic field of 500 G, and the evaluation of the fine structure required some assumptions about the 2^3P g factors. Relativistic and motional contributions to these g factors were calculated using quasihydrogenic radial wave functions. The nature of the radial integrals involved was such that the g-factor calculations contributed a significant portion of the experimental uncertainty quoted for the fine structure. For this reason, and because of an intrinsic interest in the Zeeman effect of the 2^3P state of helium, we decided to measure the g factors directly.

In this paper, we report measurements of the 2^3P g factors (including factors off diagonal in J) to a precision of about 10 ppm. These g factors occur in matrix elements of the Zeeman Hamiltonian expressed in a (J, m_J) representation. They were expressed in terms of unknown radial integrals arising from relativistic and motional contributions, and their values were deduced from measurements of a series of magnetic dipole transitions between Zeeman sublevels. A brief report of this work has been given.[2]

The relativistic contributions have been derived theoretically from the Dirac-Breit equation by Perl and Hughes.[3] A generalization for many-electron atoms was presented by Perl,[4] and by Abragam and van Vleck.[5] Several comparisons with experiment have been made utilizing this theory. The measurement[6] of g_J (He; 2^3S_1) agrees to within 1 ppm with theory,[3] where most of the relativistic contributions could be evaluated in terms of known quantities, and detailed radial wave functions were not required. In more complicated atoms, the relevant radial integrals are evaluated usually with Hartree-Fock wave functions. Detailed comparisons have been made, for instance, in the $^2P_{3/2}$ state of fluorine[7] (agreement to within 1 ppm), and in the ^3P states of oxygen[8] (agreement to 7 ppm).

The present work differs from those above in that the Zeeman transitions observed had line-